The Diaphanous-Related Formins Promote Protrusion Formation and Cell-to-Cell Spread of *Listeria monocytogenes*

Ramzi Fattouh,[1,a] Hyunwoo Kwon,[4,a] Mark A. Czuczman,[1,4] John W. Copeland,[7] Laurence Pelletier,[4,6] Margot E. Quinlan,[8] Aleixo M. Muise,[1,2,3,5] Darren E. Higgins,[9] and John H. Brumell[1,3,4,5]

[1]Cell Biology Program, [2]Division of Gastroenterology, Hepatology, and Nutrition, Department of Paediatrics, and [3]SickKids IBD Centre, Hospital for Sick Children, [4]Department of Molecular Genetics and [5]Institute of Medical Science, University of Toronto, [6]Samuel Lunenfeld Research Institute, Mount Sinai Hospital, Toronto, and [7]Department of Cellular and Molecular Medicine, University of Ottawa, Canada; [8]Department of Chemistry and Biochemistry and Molecular Biology Institute, University of California–Los Angeles; and [9]Department of Microbiology and Immunobiology, Harvard Medical School, Boston, Massachusetts

The Gram-positive bacterium *Listeria monocytogenes* is a facultative intracellular pathogen whose virulence depends on its ability to spread from cell to cell within an infected host. Although the actin-related protein 2/3 (Arp2/3) complex is necessary and sufficient for *Listeria* actin tail assembly, previous studies suggest that other actin polymerization factors, such as formins, may participate in protrusion formation. Here, we show that Arp2/3 localized to only a minor portion of the protrusion. Moreover, treatment of *L. monocytogenes*–infected HeLa cells with a formin FH2-domain inhibitor significantly reduced protrusion length. In addition, the Diaphanous-related formins 1–3 (mDia1–3) localized to protrusions, and knockdown of mDia1, mDia2, and mDia3 substantially decreased cell-to-cell spread of *L. monocytogenes*. Rho GTPases are known to be involved in formin activation. Our studies also show that knockdown of several Rho family members significantly influenced bacterial cell-to-cell spread. Collectively, these findings identify a Rho GTPase–formin network that is critically involved in the cell-to-cell spread of *L. monocytogenes*.

Keywords. *Listeria monocytogenes*; diaphanous formins; mDia1, mDia2, mDia3; protrusion; *Listeria* cell-to-cell spread; Arp2/3; HeLa cells.

Listeria monocytogenes is an enteric human pathogen and the causative agent of listeriosis, a rare but potentially life-threatening infection in newborns, elderly persons, and immunocompromised individuals [1]. As part of its life cycle, *L. monocytogenes* replicates within the cytosol of host cells, where it exploits host cell actin assembly machinery to spread to neighboring cells [2]. The bacterial factor ActA recruits and activates host cell actin-binding proteins, including the actin-related protein 2/3 (Arp2/3) complex [3–6]. Actin polymerization at the bacterium-actin interface propels these microbes through the cytoplasm [7, 8], resembling what has been described to be a "comet with a long tail" [9]. The actin filaments that make-up the so-called comet tail were found to be short and highly cross-linked [10], as is characteristic of Arp2/3-mediated actin filament construction. Ultimately, sustained actin polymerization pushes the bacterium into the host cell plasma membrane, causing membrane distension; formation of bacterial-associated finger-like membrane extensions, termed "protrusions"; and cell-to-cell spread [9].

Interestingly, analysis of electron micrographs revealed that *L. monocytogenes* protrusions comprised 2 populations of actin filaments. In the region that is proximal to the base of the bacterium, there is an array of cross-linked short filaments, whereas the remainder of the protrusion is composed of long, parallel filaments [10, 11]. The latter observation implicates the involvement of actin assembly proteins other than the Arp2/3 complex in the formation of protrusions by *L. monocytogenes*. Among the host

Received 8 May 2014; accepted 10 September 2014; electronically published 3 October 2014.

[a]R. F. and H. K. contributed equally to this work.

Correspondence: John H. Brumell, PhD, Cell Biology Program, Hospital for Sick Children, 686 Bay St, PGCRL, Room 19.9706, Toronto, Ontario, Canada M5G0A4 (john.brumell@sickkids.ca).

The Journal of Infectious Diseases® 2015;211:1185–95

DOI: 10.1093/infdis/jiu546

factors able to directly catalyze the formation of actin filaments are members of the formin family, which possess conserved formin-homology domains 1 (FH1) and FH2 [12]. In contrast to the actin filaments assembled by the Arp2/3 complex, formins drive polymerization of unbranched actin filaments [12]. Formins are ubiquitously expressed in mammalian cells and are known to play essential roles in various fundamental cell processes, including the formation of filopodia, lamellipodia, and cellular protrusions [12–15]. Moreover, efficient protrusion formation and intercellular spread of *Shigella flexneri* and *Rickettsia parkeri*, bacteria with life cycles similar to that of *L. monocytogenes*, were shown to depend on actin polymerization by formins or formin-like proteins [16, 17]. Collectively, these findings support the notion that formins may play an important role in *L. monocytogenes*–induced protrusion formation and cell-to-cell spread. However, which ones are involved and what factors may regulate them are not known.

Here, we investigated the involvement of formins in cell-to-cell spread by *L. monocytogenes*. Our findings demonstrate that the Diaphanous-related formins are involved in *L. monocytogenes*–induced protrusion formation and, in conjunction with members of the Rho GTPase family, are important facilitators of dissemination of these bacteria.

METHODS

Cell Culture and Bacterial Strains

HeLa epithelial cells were cultured in Dulbecco's modified Eagle's medium (DMEM; Hyclone) supplemented with 10% heat-inactivated fetal bovine serum (FBS; Wisent) without antibiotics at 37°C and 5% CO_2. Cells were seeded in 24-well tissue culture plates on glass coverslips at 2.5×10^4 cells/well and 5.0×10^4 cells/well for small interfering RNA (siRNA) and plasmid transfection experiments, respectively, involving direct visual analysis. Wild-type *L. monocytogenes* 10403S [18] and 10403S Δ*actA* [19] were used for infection studies as indicated.

Antibodies, Reagents, and Constructs

Details about these materials are available in the Supplementary Materials.

siRNA and Endoribonuclease-Prepared siRNA (esiRNA) Treatment

A complete listing of the siRNA and esiRNA oligos used in this study are specified in Supplementary Table 2, and details about these analyses are available in the Supplementary Materials. The efficiency of knockdown was confirmed for select factors (Supplementary Figure 1).

Bacterial Infection

L. monocytogenes were grown for approximately 16 hours in brain-heart infusion (BHI) broth at 30°C without shaking, subcultured 1:10 in BHI without antibiotics, and grown at 37°C for 2 hours with shaking (to an OD_{600} of approximately 0.3, which is equivalent to approximately 3×10^8 colony-forming units/mL). Bacterial inocula were prepared by pelleting at $10\,000 \times g$ for 1–2 minutes, washing twice, and resuspending in phosphate-buffered saline (PBS). Bacterial inocula were then diluted in DMEM without FBS. Cells were washed twice in PBS and infected at a multiplicity of infection of 100. Bacteria were centrifuged onto cells at 225*g* for 3 minutes at room temperature, and infected cells were incubated at 37°C with 5% CO_2. Sixty minutes after infection, extracellular bacteria were removed by extensive washing with PBS. Gentamicin was added to the medium to achieve a final concentration of 10 μg/mL, which was maintained throughout the duration of the experiment.

Immunofluorescence

Details about this analysis are available in the Supplementary Materials.

Microscopy and Image Preparation

Details about these techniques are available in the Supplementary Materials.

Protrusion and Comet Tail Analysis

Images of so-called primary infected cells (ie, host cells containing >50 intracellular bacteria) were acquired, and the following parameters were analyzed using Volocity: (1) number of host cells, (2) total number of bacteria, (3) number of protrusions and actin (ie, comet) tails, and (4) lengths of protrusions and actin tails. A protrusion was defined as a bacteria-associated extension of the plasma membrane that stained positive for ezrin and actin. A comet tail was defined as a bacteria-associated actin tail that stained negative for ezrin. Only protrusions and comet tails that were >1 μm long were included in the analysis.

Plaque Assay

A total of 2.0×10^5 HeLa cells were seeded per well in 6-well tissue culture plates. Cells were transfected with siRNA 24 hours later. Cells were infected with 4.0×10^4 bacteria 48 hours after transfection. After 1 hour of infection, cells were washed 3 times with PBS and were overlaid with a 0.7% agarose–DMEM mixture containing 50 μg/mL gentamicin. At 96 hours after infection, a second agarose-medium overlay containing 6% neutral red (Sigma; N2889) and 50 μg/mL gentamicin was added. After 8 hours, plaques were imaged using a Fluorchem E scanner (Proteinsimple). Plaque diameter was measured using Adobe Photoshop, and the area was calculated as $3.14159 \times [\text{diameter}/2]^2$. Plaque area was normalized to control siRNA/esiRNA-treated cells infected with wild-type bacteria for each experiment.

Western Blotting and Real-Time Reverse-Transcription Polymerase Chain Reaction Analysis

Details about these analyses are available in the Supplementary Materials.

Data Analysis

Data were analyzed using GraphPad Prism v5.0 for Mac OS X (GraphPad Software). Data are expressed as mean ± standard error of the mean. Results were analyzed using analysis of variance with a post hoc test (described in detail in the figure legends) or an unpaired *t* test. Differences were considered statistically significant at *P* values of <.05.

RESULTS

The Arp2/3 Complex Differentially Localizes Along *L. monocytogenes* Actin Comet Tails and Protrusions

The available evidence in the literature implicates the involvement of actin polymerization factors with the capacity to generate linear filaments in the formation of *L. monocytogenes* protrusions [10]. To investigate this possibility, we examined localization of Arp p34, a subunit of the Arp2/3 complex [20], to protrusions and comet tails. To this end, HeLa cells were transfected with LifeAct-RFP (to visualize F-actin) and infected for 8 hours, and then the presence of the Arp2/3 complex on protrusions and comet tails was examined by immunofluorescence analysis. The membrane-cytoskeleton linker ezrin has been shown to localize to *L. monocytogenes*–induced protrusions but not to comet tails [10, 21]. Thus, for the purpose of analysis, protrusions were identified as bacteria-associated actin tails enriched with ezrin (ie, actin$^+$ ezrin$^+$), while comet tails were identified as bacterial-associated actin tails that stained negative for ezrin (ie, actin$^+$ ezrin$^-$; Figure 1*A*). Arp p34 localized, to some extent, to all protrusions and comet tails observed (Figure 1*A*). In the case of protrusions, we noted that Arp p34 enrichment was largely limited to approximately one-third the length of the protrusion (Figure 1*B*), emanating from the bacterial-actin interface and proceeding down the tail. In contrast, Arp p34 staining was often found along the large majority, if not the entirety, of the comet tail. The reduction in Arp p34 staining among protrusions, compared with comet tails, was further confirmed on the basis of Arp p34 staining intensity measurements (data not shown).

Formins Are Required for Protrusion Formation

To ascertain whether formins may be involved in the formation of protrusions, we infected HeLa cells with *L. monocytogenes* for 8 hours and treated them with a formin FH2-domain inhibitor (SMIFH2) during the latter 4 hours of infection. Our intent was to begin treatment with SMIFH2 at a time when primary infection was fully established (ie, approximately 1 hour after infection), but protrusion formation was not overt (ie, approximately 6 hours after infection). This small-molecule inhibitor of formin FH2 domains has been shown to prevent formin-mediated actin nucleation and processive barbed-end elongation [22]. Importantly, these effects were specific to formins as this compound did not appear to interfere with Arp2/3 complex-driven processes at the dose used in our study [22]. Treatment of *L. monocytogenes*–infected HeLa cells with SMIFH2 resulted in a significant decrease in average protrusion length (Figure 2*A* and 2*G*). Although the effect was modest, treatment with the formin FH2-domain inhibitor clearly influenced the size distribution of protrusions, as nearly 70% of protrusions were <4 μm in length in the SMIFH2-treated group, compared with approximately 45% of protrusions in vehicle-control-treated infected cells (Figure 2*B*). No differences were observed in terms of protrusion frequency (ie, number of protrusions per infected host cell) between *L. monocytogenes*–infected cells treated with SMIFH2 and those treated with vehicle control (Figure 2*C*). Treatment of infected cells with SMIFH2 did not influence the average length, size distribution, or frequency of comet tails (Figure 2*D*–*F*).

mDia1, mDia2, and mDia3 Selectively Localize to Protrusions and Are Required for Efficient Cell-to-Cell Spread of *L. monocytogenes*

Given that protrusion formation is critical to *L. monocytogenes* cell-to-cell spread and that treatment with a general formin inhibitor influenced protrusion length, we sought to specifically identify the formins that may be involved in cell-to-cell spread of *L. monocytogenes*. To this end, we screened the approximately 15 mammalian formins for localization to protrusions. We transfected HeLa cells with epitope-tagged constructs of formin proteins and examined their association with protrusions in HeLa cells 8 hours after infection. Of the 15 formins we examined, only the mDia proteins were enriched along protrusions (>95% of protrusions), while none of the other formins were present above background levels on these structures (<5% of protrusions; Figure 3*A* and data not shown). In addition, mDia1-3 were rarely, if ever, observed to associate with comet tails (<5% of comets; Figure 3*B* and data not shown).

Next, we investigated whether the mDia formins were required for *L. monocytogenes* cell-to-cell spread in a plaque assay, using esiRNA. esiRNAs are a pool of siRNA-like oligonucleotides that cover a larger region of the messenger RNA being targeted for depletion. The different siRNAs that constitute this pool are present in comparable quantities and share the same on-target gene. As a result, the silencing capacity is augmented, and off-target effects are reduced [23]. Knockdown of mDia1, mDia2, and mDia3 led to a substantial reduction in plaque area, indicative of diminished cell-to-cell spread (Figure 4*A* and 4*B*).

We also examined the influence of mDia1, mDia2, and mDia3 knockdown on protrusion formation. Depletion of mDia1 and mDia3 significantly reduced the average protrusion length, while knockdown of mDia2 had only a minor, statistically insignificant effect, compared with control esiRNA–treated cells (Figure 4*C*). No differences were observed with respect to protrusion frequency, comet tail length, or comet tail frequency between any of the mDia formin-depleted groups and the control group (Figure 4*C* and data not shown).

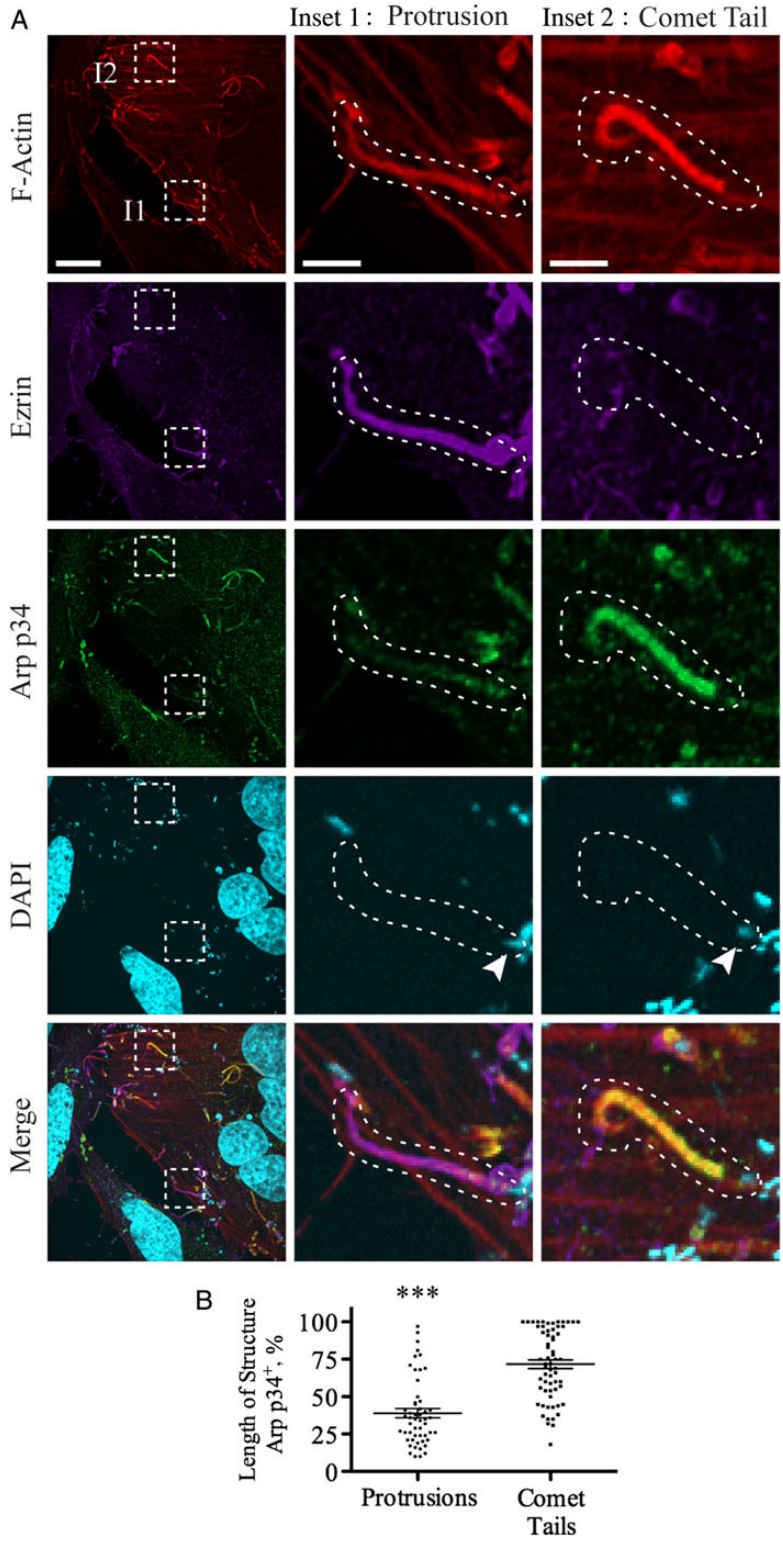

Figure 1. The actin-related protein 2/3 (Arp2/3) complex is primarily associated with comet tails. *A*, HeLa cells were transfected with LifeAct-RFP (F-actin probe), infected with *Listeria monocytogenes* for 8 hours, and immunostained with DAPI (to visualize bacteria) and antibodies to Arp p34 and ezrin. Representative confocal images are shown of a protrusion (inset 1: actin$^+$ ezrin$^+$) and comet tail (inset 2: actin$^+$ ezrin$^-$). Arrowheads denote the bacterium associated with the protrusion/comet tail identified by the dashed line. Scale bar, 10 μm for low magnification and 3 μm for I1 and I2. *B*, The length along the protrusion/comet tail demonstrating Arp p34 enrichment (based on signal thresholding) was quantified and expressed as a percentage of the total protrusion/comet tail length. Arp p34 staining was measured on at least 50 protrusions and comet tails. Data show individual measurements along with average values (± standard error of the mean). Statistical analysis was performed using an unpaired *t* test. ***$P < .001$.

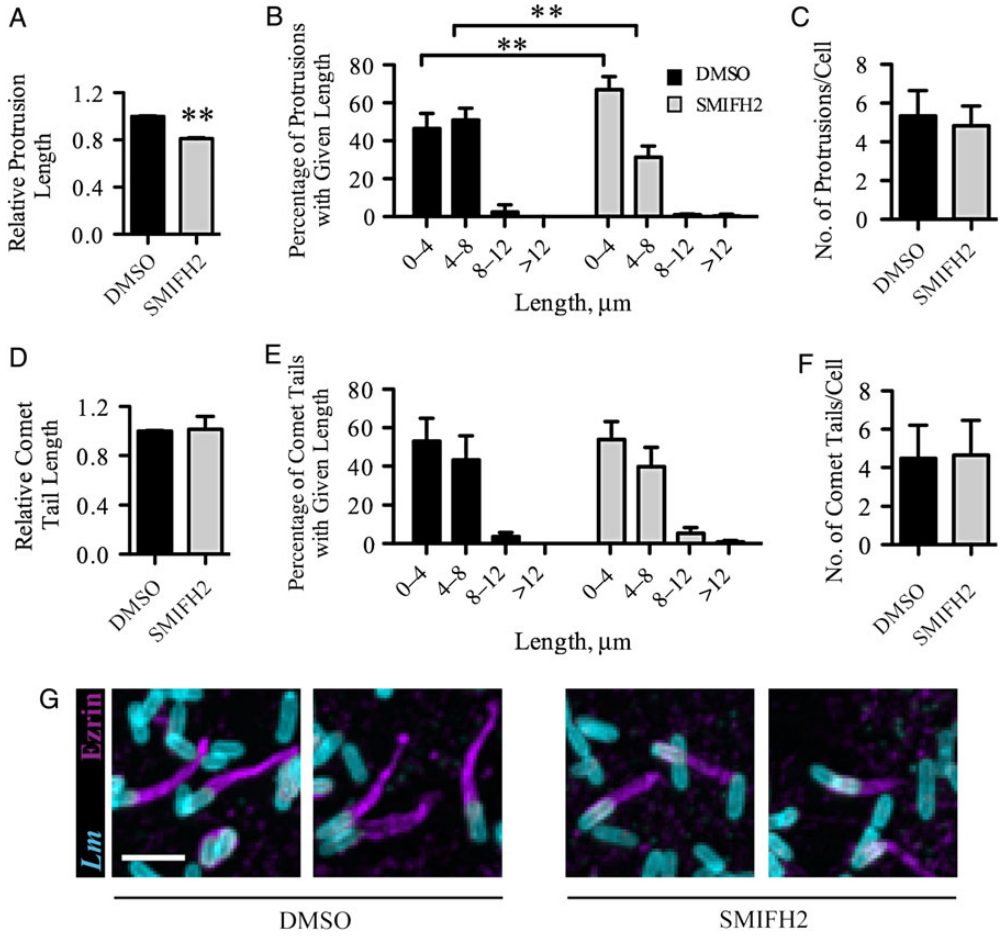

Figure 2. Treatment with small-molecule inhibitor of formin-homology domains 2 (SMIFH2) reduces the length of bacterial plasma membrane protrusions. HeLa cells were infected with *Listeria monocytogenes* and were treated with dimethyl sulfoxide (DMSO; vehicle control) or SMIFH2 (25 µM) during the latter 4 hours of an 8-hour period of infection. Cells were immunostained with antibodies against *L. monocytogenes* and ezrin and, for F-actin, with Phalloidin. *A* and *D*, Protrusion length (*A*) and comet tail length (*D*) relative to DMSO-treated cells. The average protrusion length, by treatment group, was as follows: 4.44 µm for DMSO and 3.60 µm for SMIFH2. The average comet tail length, by treatment group, was as follows: 4.18 µm for DMSO and 4.22 µm for SMIFH2. *B* and *E*, Proportion of protrusions (*B*) and comet tails (*E*) that lie within the indicated size ranges. *C* and *F*, Number of protrusions (*C*) and comet tails (*F*) per host cell. Analyses were based on images captured by spinning disk confocal microscopy. At least 75 protrusions or comet tails were measured per condition, per experiment, in panels *A, B, D,* and *E* (for DMSO-treated cells, the total number of protrusions and comets analyzed was 395 and 315, respectively; for SMIFH2-treated cells, the total number of protrusions and comets analyzed was 365 and 335, respectively), and at least 25 invaded cells were analyzed in panels *C* and *F*. *G*, Representative spinning disk confocal images are shown of protrusions treated with vehicle alone or SMIFH2. Scale bar, 3 µm. Data show average values (± standard error of the mean) for 3 independent experiments. Statistical analysis was performed using an unpaired *t* test (*A, C, D,* and *F*) and 2-way analysis of variance with the Tukey post-hoc test (*B* and *E*). $^{*}P < .05$ and $^{**}P < .01$, compared with the DMSO-treated group.

Rho GTPases Participate in *L. monocytogenes* Cell-to-Cell Spread

Several reports have demonstrated that the mDia subfamily of formins function, at least in part, as Rho GTPase effectors. Thus, in an effort to identify the involvement of Rho GTPases in *L. monocytogenes* cell-to-cell spread, we screened a limited group of Rho GTPases that have been previously implicated in mDia activation. Using siRNA, we investigated the influence of individually depleting select GTPases on *L. monocytogenes* cell-to-cell spread by plaque assay. Of the GTPases examined, knockdown of Rac1, Cdc42, RhoA, RhoC, and RhoD led to considerable decreases in plaque size (Figure 5). Treatment with siRNA against RhoB, RhoG, and Rac2 had no effect on plaque size.

DISCUSSION

The mechanisms used by *L. monocytogenes* to drive intracellular motility within an infected host cell are well understood. Comparatively less is known regarding the processes and factors involved in the formation of protrusions and cell-to-cell spread. Given that the host Arp2/3 complex is important for

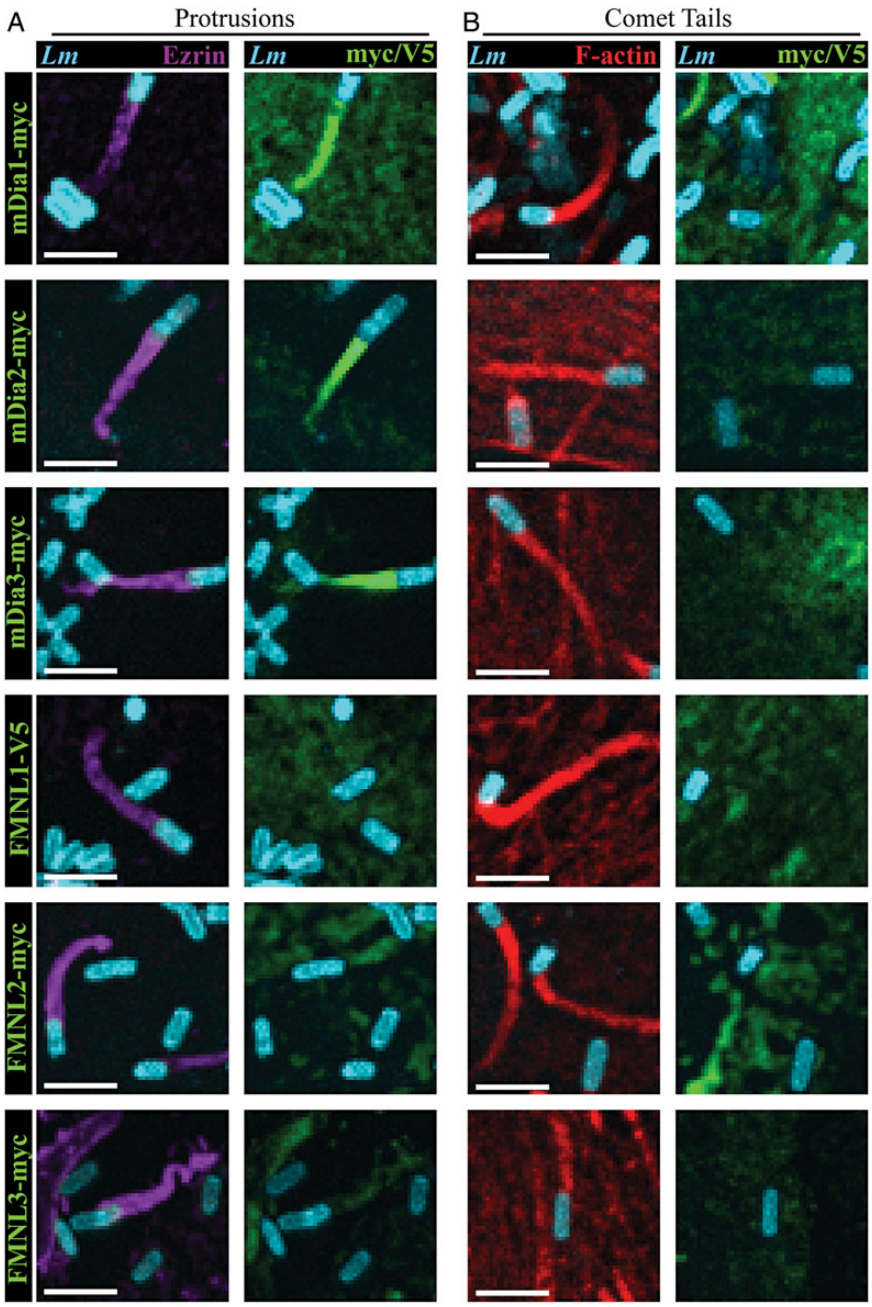

Figure 3. The formins (mDia1–3) selectively localize to protrusions. HeLa cells were transfected with mDia1-myc, mDia2-myc, mDia3-myc, FMNL1-V5, FMNL2-myc, or FMNL3-myc. Twenty-four hours after transfection, cells were subsequently infected with *Listeria monocytogenes* (*Lm*) for 8 hours and then immunostained with antibodies to *Lm*, ezrin, and myc/V5, and for F-actin, with Phalloidin. Representative spinning disk confocal images are shown of protrusions (*A*) and comet tails (*B*; left panels) and the presence/absence of the indicated formin on these structures (right panels). Scale bar, 3 μm. Images of cells transfected with FMNL constructs are shown as representative of all other formins that displayed a negative result with respect to enrichment at the protrusion.

L. monocytogenes comet tail formation and intracellular motility, we examined the localization of this complex to protrusions. In agreement with a recent report, we noted that in contrast to comet tails, where Arp2/3 is localized along the majority of the tail, this complex is enriched along a small portion of the protrusion [24], indicating to us that other host actin nucleating factors may contribute to protrusion formation.

The notion that formins are involved in the dissemination of *L. monocytogenes* is in line with previous studies that have demonstrated the importance of formins or formin-like factors

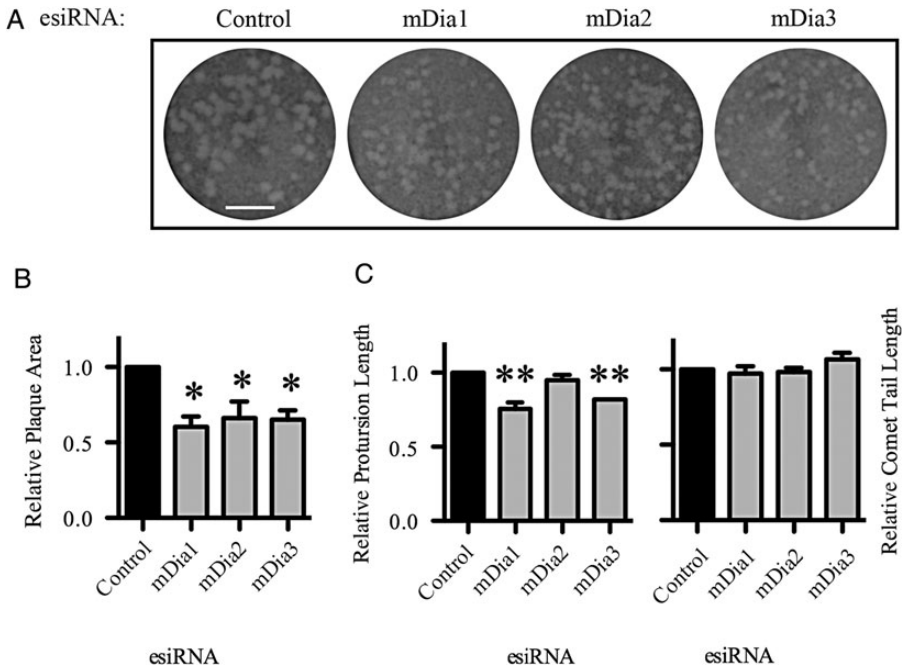

Figure 4. Knockdown of the formins mDia1, mDia2 and mDia3 (mDia1-3) reduces cell-to-cell spread of *Listeria monocytogenes* and shortens the length of bacterial plasma membrane protrusions. HeLa cells were transfected with control endoribonuclease-prepared small interfering RNA (esiRNA) or esiRNA against mDia1, mDia2, and mDia3. Forty-eight hours after transfection, cells were infected with *L. monocytogenes*, and a plaque assay was performed as described in Materials and Methods. *A*, Representative images of the plaque assay. Scale bar, 1 cm. *B*, Data show the average plaque area relative to control esiRNA-treated plaques (± standard error of the mean [SEM]) of 3 independent experiments. Average plaque areas, by treatment group, were as follows: 9.73 mm^2 for control, 5.86 mm^2 for mDia1, 6.43 mm^2 for mDia2, and 6.37 mm^2 for mDia3. Statistical analysis was performed using 1-way analysis of variance (ANOVA) with the Dunnett multiple comparison post-hoc test. **P* < .05, compared with the control esiRNA-transfected group. *C*, Forty-eight hours after transfection, cells were infected with *L. monocytogenes* and fixed 8 hours after infection. Cells were then immunostained with antibodies against *L. monocytogenes* and ezrin and, for F-actin, with Phalloidin. Analysis of protrusion and comet tail length relative to control esiRNA-treated cells was based on images captured by spinning disk confocal microscopy. At least 75 protrusions or comet tails were measured per condition, per experiment. The total number of protrusions analyzed was as follows: 330 for control, 360 for mDia1, 390 for mDia2, and 385 for mDia3. The total number of comet tails analyzed, by treatment group, was as follows: 540 for control, 590 for mDia1, 770 for mDia2, and 530 for mDia3. Data are average values (± SEM) for 3 independent experiments. The average protrusion length, by treatment group, was as follows: for 4.76 μm for control, 3.61 μm for mDia1, 4.51 μm for mDia2, and 3.90 μm for mDia3. The average comet tail length, by treatment group, was as follows: 5.25 μm for control, 5.10 μm for mDia1, 5.10 μm for mDia2, and 5.37 μm for mDia3. Statistical analysis was performed using 1-way ANOVA with the Tukey post-hoc test. **P* < .05 and ***P* < .01, compared with the control esiRNA–treated group.

in the spread of various other human pathogens. Indeed, FHOD1 has recently been shown to facilitate robust actin-based motility of host-cell extracellular-associated vaccinia viral particles, leading to protrusion formation and dissemination to neighboring cells in vitro [25]. Notably, recruitment of FHOD1 and its involvement in actin tail formation was shown to be dependent on Rac1 activity [25]. In addition, the surface cell antigen 2 (Sca2) of *Rickettsia* is critically required for actin-tail formation and virulence [26]. Of significance, Sca2 functions, similarly to eukaryotic formins, as a profilin-dependent barbed-end elongation factor that directly mediates polymerization of host actin into unbranched filaments [17] to propel bacteria throughout the host cell. In the case of *S. flexneri*, studies performed by Heindl et al showed that, upon depletion of mDia1 and mDia2, the frequency of protrusions was decreased relative to controls and that this effect was associated with impaired spread [16]. Codepletion of mDia1 and mDia2 did not further influence protrusion formation. In contrast, we did not observe a difference in the number of protrusions formed following treatment of *L. monocytogenes*–infected HeLa cells with either an FH2-inhibitor or an esiRNA against mDia1–3. These findings suggest that, in the context of *L. monocytogenes*, other factors in addition to formins may participate in protrusion elongation and that the initiation of these structures may not be impaired by formin inhibition. As neither SMIFH2 treatment nor mDia1–3 esiRNA influenced comet tail length or number, perhaps it is not unexpected that *L. monocytogenes* was able to contact the plasma membrane and initiate protrusion assembly to the same extent as in control-treated cells. Interestingly, although it did not reach statistical significance,

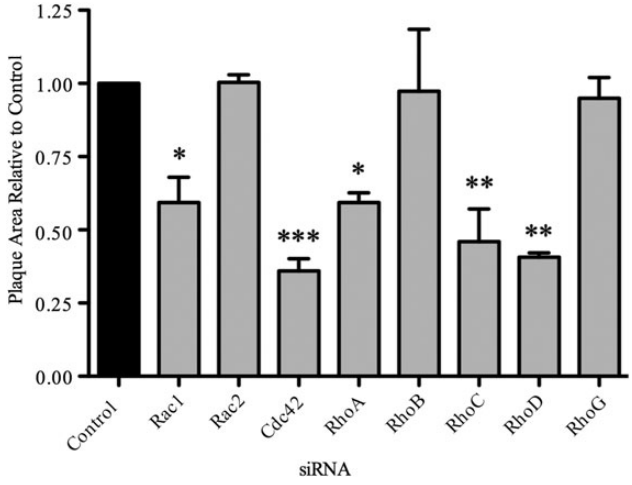

Figure 5. Knockdown of select Rho GTPases reduces cell-to-cell spread of *Listeria monocytogenes*. HeLa cells were transfected with control small interfering RNA (siRNA) or siRNA against the indicated Rho GTPases. Forty-eight hours after transfection, cells were infected with *L. monocytogenes*, and a plaque assay was performed as described in Materials and Methods. Data show the average plaque area relative to control siRNA-treated plaques (± standard error of the mean) for 3 independent experiments. The average plaque areas, by treatment group, were as follows: 5.93 mm^2 for control, 3.50 mm^2 for Rac1, 5.95 mm^2 for Rac2, 2.14 mm^2 for Cdc42, 3.50 mm^2 for RhoA, 5.77 mm^2 for RhoB, 2.72 mm^2 for RhoC, 2.41 mm^2 for RhoD, and 5.63 mm^2 for RhoG. Statistical analysis was performed using 1-way analysis of variance with the Dunnett multiple comparison post-hoc test. *P < .05, **P < .01, and ***P < .001, compared with the control siRNA–transfected group.

inhibition of mDia1 or mDia2 showed a trend toward decreased *Shigella* actin tail length within the host cell body (ie, comets), indicating that, in addition to their involvement in protrusions, these formins may also participate in the assembly of *Shigella* comet tails [16]. Therefore, mDia proteins may influence *Shigella* cell-to-cell spread by regulating protrusion frequency and, perhaps, comet tail length, while in the case of *L. monocytogenes*, mDia proteins may facilitate cell-to-cell spread by mediating protrusion elongation.

At present, the possibility that mDia inhibition indirectly influenced *L. monocytogenes* cell spread in some fashion, such as by affecting cell-cell interactions, cannot be excluded. However, the reduction in protrusion length following targeted depletion of mDia1, mDia3, and, to a small extent, mDia2, coupled with the observation that mDia formins localize to protrusions, argues against the contribution of indirect effects. Moreover, decreased protrusion length has been previously shown to correlate with reduced cell-to-cell spread [27].

Yeast 2-hybrid-based analyses conducted over a decade ago identified mDia family members as downstream effectors of the Rho family of small GTPases [28, 29]. Binding of activated Rho proteins to the Rho GTPase–binding domain of mDia formins induces these formins to nucleate and polymerize actin [12]. Since these discoveries, a network of interactions between these 2 groups of proteins has been described, and various processes were shown to involve cooperation between Rho GTPases and mDia proteins [29–34] including, stress fiber formation, vesicle movement, and filopodia and lamellipodia protrusion [13, 22, 30, 34–38]. To begin to discover the potential network of Rho GTPases that may be involved in *L. monocytogenes* cell-to-cell spread, we screened a subset of the Rho GTPase family by using a conventional plaque assay. Several of the GTPases screened proved to be required for efficient cell-to-cell spread. Our observation that Cdc42 knockdown led to diminished *L. monocytogenes* spread is, seemingly, in disagreement with a previous report [39]. Rigano et al noted that efficient protrusion formation and spread of *Listeria* required the effector protein internalin C (InlC), which mediated the downregulation of activated Cdc42. Of significance, there were several well-recognized differences among the methods used that could account for these discordant results. Overexpression of a dominant-negative construct was used by Rigano et al to interfere with Cdc42, and their studies were conducted in the context of a polarized cell-line (Caco-2 BBE1 cells), whereas we used an siRNA-based approach and a nonpolarized cell line (HeLa cells). Alternatively, it is conceivable that *Listeria* drives local inhibition of Cdc42 at sites where InlC or other virulence factors are localized. But there may be a general requirement for Cdc42 (eg, for trafficking processes) at other cellular sites that are required for productive spread. On the basis of the experimental approach used here, we cannot rule out the possibility that some of the GTPases we examined may affect cell-to-cell spread through involvement in 1 or more events upstream and/or downstream of protrusion formation (eg, invasion, comet tail formation, and uptake of *L. monocytogenes* protrusions by neighboring uninfected host cells). It is worth noting that the findings of some studies, but not all, suggest that select Rho GTPases may play a role in promoting *L. monocytogenes* invasion, although perhaps not intracellular motility [40–45]. Noteworthy, the evidence suggests that involvement of Rho GTPases in these processes may depend, in part, on the cell type examined and the mechanism of invasion used by *L. monocytogenes*.

It is becoming increasingly clear that the formation of membrane protrusions by *L. monocytogenes* and related pathogens is an active process and not simply a byproduct of the forces generated by actin-based cytosolic propulsion. Indeed, *Escherichia coli* expressing IcsA, the molecule that is necessary and sufficient for *Shigella* actin-based motility, was adequate to promote protrusion formation in a manner that was largely related to the direction but not the speed of intracellular travel [46]. This finding is evidence that a primary objective of intracellular motility may be to contact the membrane and not necessarily to provide the forces required to project through it. This is not to say that the

force of contact is not an important factor for protrusion formation, but rather that it is not likely to be the sole contributing factor determining whether a protrusion develops. In this regard, disruption of ezrin, a key membrane-cytoskeleton linker that accumulates at *L. monocytogenes*–induced protrusions, specifically reduces the number and morphology (shortened and collapsed) of protrusions, resulting in impaired cell-to-cell spread [21]. Myosin-X has also been shown to play a critical role in the development of protrusions [27]. As a consequence of Myo10 depletion, *Shigella* protrusions were stunted, and cell-to-cell spread was dramatically diminished. Myo10 was observed to concentrate at the base of *Shigella* and to cycle along its sides within a protrusion as the protrusion lengthened. Similarly, Myo10 accumulated in *L. monocytogenes*–induced protrusions, and knockdown of this protein also impaired bacterial cell-to-cell spread [27]. In addition, InlC of *L. monocytogenes* has been shown to facilitate protrusion formation by regulating cell membrane tension [47]. InlC was found to interfere with the interaction between the mammalian adaptor protein Tuba and the actin regulator N-WASP2, which together regulate cortical actin tension at apical junctions. Disruption of the Tuba-N-WASP interaction by binding of InlC to Tuba, via a C-terminal SH3 domain, resulted in a loss of membrane tension, creating slack that permits protrusion formation by *L. monocytogenes*. Disruption of components of the host cell actin network disassembly machinery has also been reported to impair *L. monocytogenes* spread. Specifically, codepletion of actin-interacting protein 1 and cofilin 1 dramatically reduced the velocity of *Listeria* in protrusions, led to altered protrusion morphology, and decreased bacterial spread to adjacent uninfected host cells [24]. Collectively, these findings strongly suggest that bacterial effector proteins in conjunction with host cell factors actively drive the formation of bacterial-associated protrusions.

The observations presented here identify a potential network of formins and Rho GTPases that aid in active protrusion formation (Figure 6). *L. monocytogenes* forms ActA- and Arp2/3-dependent comet tails within the host cell cytoplasm [2, 5, 6]. Similar to the involvement of N-WASP and FHOD1-Rac1 pathways in the spread of vaccinia virus [25], processes related to actin-based motility and/or contact with the cell membrane may activate Rho GTPases, which, in turn, recruit and induce the activation of formins, such as mDia1–3. Subsequently, these mDia proteins contribute to the elongation of actin filaments in protrusions, independent of Arp2/3, thereby promoting *L. monocytogenes* cell-to-cell spread. Thus, our findings show that *L. monocytogenes* exploits the mDia subfamily of formins to promote effective cell-to-cell spread. Characterization of the precise array of host factors involved specifically in the protrusion phase may help to identify novel strategies through which the spread and resulting pathologies of intracellular pathogens such as *L. monocytogenes* can be abrogated.

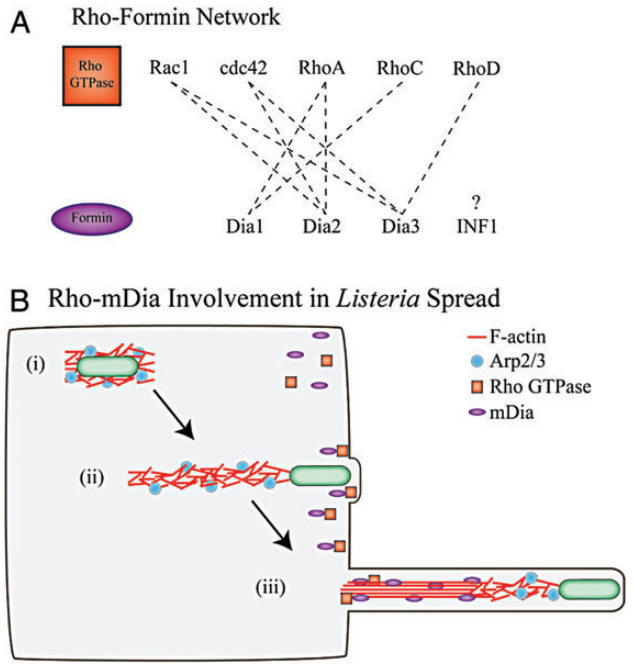

Figure 6. Schematic model outlining the putative involvement of a Rho GTPase–formin network in the formation of *Listeria monocytogenes*–induced protrusions and cell-to-cell spread. *A*, Illustrates the network of Rho GTPase–Diaphanous-related formin (mDia) interactions potentially involved in *L. monocytogenes* cell-to-cell spread. Interactions between Rho GTPases and mDia proteins (ie, dashed lines) are based on previously published studies [35]. *B*, Following entry and escape from the host cell phagosome, *L. monocytogenes* uses its ActA protein (not shown) to recruit the host cell actin polymerization complex, Arp2/3 (i). Arp2/3-mediated actin polymerization provides the propulsive force that drives *L. monocytogenes* intracellular motility, facilitating contact with the plasma membrane (ii). Activation of Rho GTPases leads to binding and activation of the mDia formins that, in turn, catalyze the formation of unbranched actin filaments to assist in the formation of *L. monocytogenes* protrusions (iii).

Supplementary Data

Supplementary materials are available at *The Journal of Infectious Diseases* online (http://jid.oxfordjournals.org). Supplementary materials consist of data provided by the author that are published to benefit the reader. The posted materials are not copyedited. The contents of all supplementary data are the sole responsibility of the authors. Questions or messages regarding errors should be addressed to the author.

Notes

Acknowledgments. We thank Mike Woodside and Paul Paroutis for their support with microscopy.

Financial support. This work was supported by the Arthritis Society of Canada (grant RG11/013 to J. H. B.); the US Public Health Service (grant AI053669 from the National Institutes of Health to D. E. H.); the Hospital for Sick Children (Pitblado Chair in Cell Biology to J. H. B.); the Canadian Institutes of Health Research, in partnership with the Canadian Association of Gastroenterology and the Crohn's and Colitis Foundation of Canada (postdoctoral fellowship to R. F.); the Research Training Committee, Hospital for Sick Children (studentship to M. A. C.); the University of Toronto

(Open Fellowship to M. A. C.); the Canada Graduate Scholarships–Master's Program, Natural Science and Engineering Research Council of Canada (scholarship to M. A. C.); a Canada Research Chair in Centrosome Biogenesis and Function (tier 2; to L. P.); and the Ontario Research Fund Global Leadership Round in Genomics and Life Sciences (for support of the esiRNA pipeline).

Potential conflicts of interest. All authors: No reported conflicts.

All authors have submitted the ICMJE Form for Disclosure of Potential Conflicts of Interest. Conflicts that the editors consider relevant to the content of the manuscript have been disclosed.

References

1. Lecuit M. Human listeriosis and animal models. Microbes Infect **2007**; 9:1216–25.
2. Stavru F, Archambaud C, Cossart P. Cell biology and immunology of *Listeria monocytogenes* infections: novel insights. Immunol Rev **2011**; 240:160–84.
3. Domann E, Wehland J, Rohde M, et al. A novel bacterial virulence gene in *Listeria monocytogenes* required for host cell microfilament interaction with homology to the proline-rich region of vinculin. EMBO J **1992**; 11:1981–90.
4. Kocks C, Gouin E, Tabouret M, Berche P, Ohayon H, Cossart P. *L. monocytogenes*-induced actin assembly requires the actA gene product, a surface protein. Cell **1992**; 68:521–31.
5. Welch MD, Iwamatsu A, Mitchison TJ. Actin polymerization is induced by Arp2/3 protein complex at the surface of *Listeria monocytogenes*. Nature **1997**; 385:265–9.
6. Welch MD, Rosenblatt J, Skoble J, Portnoy DA, Mitchison TJ. Interaction of human Arp2/3 complex and the *Listeria monocytogenes* ActA protein in actin filament nucleation. Science **1998**; 281:105–8.
7. Sanger JM, Sanger JW, Southwick FS. Host cell actin assembly is necessary and likely to provide the propulsive force for intracellular movement of *Listeria monocytogenes*. Infect Immun **1992**; 60:3609–19.
8. Theriot JA, Mitchison TJ, Tilney LG, Portnoy DA. The rate of actin-based motility of intracellular *Listeria monocytogenes* equals the rate of actin polymerization. Nature **1992**; 357:257–60.
9. Tilney LG, Portnoy DA. Actin filaments and the growth, movement, and spread of the intracellular bacterial parasite, *Listeria monocytogenes*. J Cell Biol **1989**; 109:1597–608.
10. Sechi AS, Wehland J, Small JV. The isolated comet tail pseudopodium of *Listeria monocytogenes*: a tail of two actin filament populations, long and axial and short and random. J Cell Biol **1997**; 137:155–67.
11. Gouin E, Gantelet H, Egile C, et al. A comparative study of the actin-based motilities of the pathogenic bacteria *Listeria monocytogenes*, Shigella flexneri and Rickettsia conorii. J Cell Sci **1999**; 112(Pt 11): 1697–708.
12. Campellone KG, Welch MD. A nucleator arms race: cellular control of actin assembly. Nat Rev Mol Cell Biol **2010**; 11:237–51.
13. Koizumi K, Takano K, Kaneyasu A, et al. RhoD activated by fibroblast growth factor induces cytoneme-like cellular protrusions through mDia3C. Mol Biol Cell **2012**; 23:4647–61.
14. Mellor H. The role of formins in filopodia formation. Biochim Biophys Acta **2010**; 1803:191–200.
15. Yang C, Czech L, Gerboth S, Kojima S, Scita G, Svitkina T. Novel roles of formin mDia2 in lamellipodia and filopodia formation in motile cells. PLoS Biol **2007**; 5:e317.
16. Heindl JE, Saran I, Yi CR, Lesser CF, Goldberg MB. Requirement for formin-induced actin polymerization during spread of Shigella flexneri. Infect Immun **2010**; 78:193–203.
17. Haglund CM, Choe JE, Skau CT, Kovar DR, Welch MD. Rickettsia Sca2 is a bacterial formin-like mediator of actin-based motility. Nat Cell Biol **2010**; 12:1057–63.
18. Bishop DK, Hinrichs DJ. Adoptive transfer of immunity to *Listeria monocytogenes*. The influence of in vitro stimulation on lymphocyte subset requirements. J Immunol **1987**; 139:2005–9.
19. Skoble J, Portnoy DA, Welch MD. Three regions within ActA promote Arp2/3 complex-mediated actin nucleation and *Listeria monocytogenes* motility. J Cell Biol **2000**; 150:527–38.
20. Robinson RC, Turbedsky K, Kaiser DA, et al. Crystal structure of Arp2/3 complex. Science **2001**; 294:1679–84.
21. Pust S, Morrison H, Wehland J, Sechi AS, Herrlich P. *Listeria monocytogenes* exploits ERM protein functions to efficiently spread from cell to cell. EMBO J **2005**; 24:1287–300.
22. Rizvi SA, Neidt EM, Cui J, et al. Identification and characterization of a small molecule inhibitor of formin-mediated actin assembly. Chem Biol **2009**; 16:1158–68.
23. Theis M, Buchholz F. High-throughput RNAi screening in mammalian cells with esiRNAs. Methods **2011**; 53:424–9.
24. Talman AM, Chong R, Chia J, Svitkina T, Agaisse H. Actin network disassembly powers dissemination of *Listeria monocytogenes*. J Cell Sci **2014**; 127:240–9.
25. Alvarez DE, Agaisse H. The formin FHOD1 and the small GTPase Rac1 promote vaccinia virus actin-based motility. J Cell Biol **2013**; 202:1075–90.
26. Kleba B, Clark TR, Lutter EI, Ellison DW, Hackstadt T. Disruption of the Rickettsia rickettsii Sca2 autotransporter inhibits actin-based motility. Infect Immun **2010**; 78:2240–7.
27. Bishai EA, Sidhu GS, Li W, et al. Myosin-X facilitates Shigella-induced membrane protrusions and cell-to-cell spread. Cell Microbiol **2013**; 15:353–67.
28. Alberts AS, Bouquin N, Johnston LH, Treisman R. Analysis of RhoA-binding proteins reveals an interaction domain conserved in heterotrimeric G protein beta subunits and the yeast response regulator protein Skn7. J Biol Chem **1998**; 273:8616–22.
29. Watanabe N, Madaule P, Reid T, et al. p140mDia, a mammalian homolog of Drosophila diaphanous, is a target protein for Rho small GTPase and is a ligand for profilin. EMBO J **1997**; 16:3044–56.
30. Gasman S, Kalaidzidis Y, Zerial M. RhoD regulates endosome dynamics through Diaphanous-related Formin and Src tyrosine kinase. Nat Cell Biol **2003**; 5:195–204.
31. Lammers M, Meyer S, Kuhlmann D, Wittinghofer A. Specificity of interactions between mDia isoforms and Rho proteins. J Biol Chem **2008**; 283:35236–46.
32. Peng J, Wallar BJ, Flanders A, Swiatek PJ, Alberts AS. Disruption of the Diaphanous-related formin Drf1 gene encoding mDia1 reveals a role for Drf3 as an effector for Cdc42. Curr Biol **2003**; 13:534–45.
33. Rose R, Weyand M, Lammers M, Ishizaki T, Ahmadian MR, Wittinghofer A. Structural and mechanistic insights into the interaction between Rho and mammalian Dia. Nature **2005**; 435:513–8.
34. Watanabe N, Kato T, Fujita A, Ishizaki T, Narumiya S. Cooperation between mDia1 and ROCK in Rho-induced actin reorganization. Nat Cell Biol **1999**; 1:136–43.
35. Goh WI, Ahmed S. mDia1-3 in mammalian filopodia. Commun Integr Biol **2012**; 5:340–4.
36. Goh WI, Lim KB, Sudhaharan T, et al. mDia1 and WAVE2 proteins interact directly with IRSp53 in filopodia and are involved in filopodium formation. J Biol Chem **2012**; 287:4702–14.
37. Wallar BJ, Deward AD, Resau JH, Alberts AS. RhoB and the mammalian Diaphanous-related formin mDia2 in endosome trafficking. Exp Cell Res **2007**; 313:560–71.
38. Zaoui K, Honore S, Isnardon D, Braguer D, Badache A. Memo-RhoA-mDia1 signaling controls microtubules, the actin network, and adhesion site formation in migrating cells. J Cell Biol **2008**; 183:401–8.
39. Rigano LA, Dowd GC, Wang Y, Ireton K. *Listeria monocytogenes* antagonizes the human GTPase Cdc42 to promote bacterial spread. Cell Microbiol **2014**; 16:1068–79.
40. Bosse T, Ehinger J, Czuchra A, et al. Cdc42 and phosphoinositide 3-kinase drive Rac-mediated actin polymerization downstream of c-Met in distinct and common pathways. Mol Cell Biol **2007**; 27:6615–28.
41. Ebel F, Rohde M, von Eichel-Streiber C, Wehland J, Chakraborty T. The actin-based motility of intracellular *Listeria monocytogenes* is not controlled by small GTP-binding proteins of the Rho- and Ras-subfamilies. FEMS Microbiol Lett **1999**; 176:117–24.

42. Gavicherla B, Ritchey L, Gianfelice A, Kolokoltsov AA, Davey RA, Ireton K. Critical role for the host GTPase-activating protein ARAP2 in InlB-mediated entry of *Listeria monocytogenes*. Infect Immun **2010**; 78:4532–41.
43. Ireton K, Rigano LA, Dowd GC. Role of host GTPases in infection by *Listeria monocytogenes*. Cell Microbiol **2014**; 16:1311–20.
44. Kirchner M, Higgins DE. Inhibition of ROCK activity allows InlF-mediated invasion and increased virulence of *Listeria monocytogenes*. Mol Microbiol **2008**; 68:749–67.
45. Moreau V, Way M. Cdc42 is required for membrane dependent actin polymerization in vitro. FEBS Lett **1998**; 427:353–6.
46. Monack DM, Theriot JA. Actin-based motility is sufficient for bacterial membrane protrusion formation and host cell uptake. Cell Microbiol **2001**; 3:633–47.
47. Rajabian T, Gavicherla B, Heisig M, et al. The bacterial virulence factor InlC perturbs apical cell junctions and promotes cell-to-cell spread of Listeria. Nat Cell Biol **2009**; 11:1212–8.